The Astrophysical Journal Supplement Series, 144:287–297, 2003 February

ROTATIONAL SPECTRA OF THE NITROGEN-SULFUR CARBON CHAINS NC_nS, $n = 1$–7

M. C. McCarthy,[1] A. L. Cooksy,[2] S. Mohamed,[1] V. D. Gordon,[1] and P. Thaddeus[1]

Received 2002 August 14; accepted 2002 September 16

ABSTRACT

Seven carbon chain radicals NC_nS where $n = 1$–7 have been detected in a supersonic molecular beam by Fourier transform microwave spectroscopy. Although NCCS is found to have a bent structure and an asymmetric top spectrum, the five longer chains have linear heavy-atom backbones, and like the isovalent HC_nS chains, the electronic ground states of each alternate with even and odd numbers of carbon atoms: NC_4S and NC_6S have $^2\Pi_{1/2}$ ground states, while NC_3S, NC_5S, and NC_7S have $^2\Pi_{3/2}$ ground states. In addition, the lowest-rotational transitions of the NCS radical have been detected in both fine-structure levels in the same supersonic molecular beam source, allowing a precise determination of the ground state hyperfine coupling constants. The centimeter-wave spectra of NC_3S and the four longer chains have been fully characterized, and spectroscopic constants, including those that describe the lambda-type doubling and hyperfine structure from the nitrogen nucleus, have been determined to high precision. A complete account of the centimeter-wave spectrum of NCCS will be given by Nakajima et al. Predicted properties from UQCISD/cc-pVDZ ab initio calculations are also reported for the NC_nS chains up to NC_7S. All six new chains are highly polar and all are plausible candidates for astronomical detection because C_nS chains up to C_3S and C_nN chains up to C_5N are detected in both interstellar and circumstellar sources.

Subject headings: ISM: molecules — line: identification — methods: laboratory — molecular data — molecular processes — radio lines: ISM

1. INTRODUCTION

Nitrogen and sulfur are two of the most cosmically abundant reactive elements. Direct evidence for their important role in the chemistry of interstellar and circumstellar sources is the detection there of more than 20 carbon chains terminated with at least one of these heteroatoms. Carbon chains of the form NC_nS, terminated at one end with a nitrogen and at the other with a sulfur, are plausible candidates for detection by radio astronomers because they possess similar structure and elemental composition to the known astronomical C_nS (Yamamoto et al. 1987, and references therein) and C_nN chains (Guélin, Neininger, & Cernicharo 1998, and references therein), and because simple nitrogen-sulfur molecules such as NS (Gottlieb et al. 1975; Kuiper et al. 1975) and HNCS (Frerking, Linke, & Thaddeus 1979) have also been found in space with radio telescopes. The polarity of the NC_nS molecules is expected to increase with chain length, providing an additional incentive for an astronomical search.

Here we present the laboratory detection of six new nitrogen-sulfur–bearing carbon chains: NC_2S through NC_7S. All but NCCS are found to possess linear heavy-atom backbones and $^2\Pi$ electronic ground states; those with an odd number of carbon atoms have inverted fine structure with the $^2\Pi_{3/2}$ state lowest in energy, while those with an even number of carbon atoms have regular fine structure with the $^2\Pi_{1/2}$ state the lowest. NCCS is found to have a bent ground-state geometry and a rotational spectrum characteristic of an asymmetric top. Strong hyperfine-split transitions from both fine-structure rotational ladders of the shorter chain NCS have also been observed, even though its $^2\Pi_{1/2}$ ladder lies more than 450 K above the $^2\Pi_{3/2}$ ladder. From measurements of the lowest rotational transitions, it has been possible to determine a complete set of ground state hyperfine coupling constants.

The six new chains here and NCS were detected by Fourier transform microwave (FTM) spectroscopy in a supersonic molecular beam. From four to 14 rotational transitions of NCCS and the five longer chains have been measured between 5 and 40 GHz, including all of the rare isotopic species of NCCS and the ^{34}S species of NC_3S, NC_4S, and NC_5S. During the course of the present work, we learned that NCCS had also been detected by M. Nakajima et al. (2003, in preparation) using a FTM spectrometer similar to ours. A complete account of the NCCS spectrum, including an analysis of the rotational and hyperfine structure, will be provided by these authors; details of the isotopic spectra and a precise determination of the NCCS molecular structure will be presented elsewhere. For NC_3S and most of the longer chains, the derived spectroscopic constants are adequate to predict the astronomically most interesting rotational transitions to better than 1 km s^{-1} in equivalent radial velocity up to 100 GHz.

2. EXPERIMENT

The same FTM spectrometer used to detect the rotational spectra of many new carbon chains and other reactive molecules during the past 6 years, including 12 sulfur-bearing carbon chains (Gordon et al. 2001, 2002), was used in the present investigation. The spectrometer and the supersonic molecular beam discharge nozzle have been described in previous publications (McCarthy et al. 1997, 2000). Briefly, a pulsed supersonic molecular beam of an organic precursor vapor heavily diluted in an inert gas is produced by a commercial solenoid valve. Many types of reactive molecules

[1] Harvard-Smithsonian Center for Astrophysics, 60 Garden Street, Cambridge, MA 02138, and Division of Engineering & Applied Sciences, Harvard University, 29 Oxford Street, Cambridge, MA 02138.

[2] Department of Chemistry, San Diego State University, 5500 Campanile Drive, San Diego, CA 92182.

are efficiently formed by applying a small electrical discharge in the throat of the supersonic nozzle, prior to adiabatic expansion. As the gas expands into the large Fabry-Perot cavity of the spectrometer, the molecules are rapidly cooled by collisions with the supersonic but kinetically cold inert gas to a fairly uniform rotational temperature of 2–3 K. When the gas fills the cavity, a short (1 μs) pulse of microwave radiation irradiates the molecules, and the subsequent free induction decay is detected with a sensitive microwave receiver. The spectrometer operates from 5 to 43 GHz and is fully computer controlled to the point where automated scans covering a wide range of frequencies or requiring many hours of integration, or both, can be conducted with little or no oversight. Rotational lines of known molecules are routinely monitored for calibration.

Since no ab initio geometries were available to guide laboratory searches for the new chains here, these were initially based on rotational constants calculated from the theoretical geometries of the C_nS chains (Lee 1997) by substituting a nitrogen atom for the terminal carbon atom in each species. The derived rotational constants were then scaled by the ratio of the experimental B value (Amano & Amano 1991) to that calculated for NCS. Rotational transitions predicted in this way turned out to be fairly accurate: to better than 2% for all but NCCS. Since no lines were found at the expected frequencies for this radical, ab initio calculations at several levels of theory were performed to better estimate its ground state geometry and rotational constants and those of longer chains up to NC_7S in the series.

The structures of linear and bent NCCS and NC_4S were predicted at the UQCISD level and compared to ROHF-based CI calculations, but only Hartree-Fock and UQCISD calculations have been carried out for the other NC_nS chains. Because sulfur is a relatively heavy atom and because the degree of the π conjugation is expected to be significant in these chains, single-reference ab initio calculations may be inaccurate owing to the high density of low-lying electronic states. In fact, spin contamination of the unrestricted Hartree-Fock wavefunction is extremely high in the series NC_nS with $n = 2$–7; $\langle S^2 \rangle$ values are as high as 1.6 for NCCS and roughly 2.5 for NC_6S and NC_7S. This degree of contamination is substantially worse than typical UHF-based coupled cluster calculations of other π-conjugated radicals of similar length, for which the predicted geometries and relative energies are in good agreement with the available experimental data. The UHF-based coupled cluster methods are nevertheless worth doing for the smaller chains here because rotational constants so calculated apparently converge much more rapidly than those done by ROHF-based methods, even when $\langle S^2 \rangle$ values reached 1.5 for the UHF reference wavefunction (Wong & Radom 1995; Parker & Cooksy 1999). Furthermore, MCSCF calculations on NC_4S with active spaces up to the full 13 electron π system—although immune to spin contamination—persist in predicting a bent geometry to be lowest in energy in apparent contradiction to the present experiments, whereas the UHF-based CI calculations correctly predict a linear geometry to be lowest in energy.

On the basis of extensive convergence tests of similar radicals (see e.g., Cooksy 2001), we have used Dunning's cc-pVDZ basis set for all of the calculations here, with occasional use of the cc-pVTZ basis set for extrapolation. The UHF-based calculations were carried out using Gaussian 98 (Frisch et al. 1998), and the ROHF-based were carried out using Gamess (Schmidt et al. 1993).

Geometries and dipole moments for NCCS through NC_7S, predicted from QCISD/cc-pVDZ calculations, are presented in Table 1 along with $\langle S^2 \rangle$ values for the corresponding reference UHF wavefunction. ROHF-based calculations are in qualitative agreement with the QCISD results, except for NC_4S, which is predicted by ROHF to be nonlinear with a CCS angle of 147°.8. In both even and odd n species, there is little qualitative difference in the predicted bond structure at the nitrogen end: the CN bond is predicted to be essentially a triple bond, and the connected carbon chain has the characteristic bond order alternation of a polyyne, but with increasing cumulenic character toward the sulfur atom.

Unlike NCS and most of the longer chains, NCCS is predicted ab initio (see Table 1) to possess a $^2A'$ ground state and a nonlinear backbone, with the CCS angle calculated to be 143° as shown in Figure 1; as a result, the expected rotational spectrum is that of a prolate asymmetric top, characterized by a series of nearly harmonically related lines with

TABLE 1

QCISD/cc-pVDZ Optimized Geometries, Dipole Moments, and UHF Reference $\langle S^2 \rangle$ Values for the NC_nS, $n = 2$–7 Chains

Parameter	NC_2S ($^2A'$)	NC_2S ($^2\Pi$)	NC_3S ($^2\Pi$)	NC_4S ($^2\Pi$)	NC_5S ($^2\Pi$)	NC_6S ($^2\Pi$)	NC_7S ($^2\Pi$)
r_{NC} (Å)	1.176	1.187	1.176	1.178	1.172	1.174	1.170
r_{CC} (Å)	1.417	1.368	1.388	1.386	1.399	1.395	1.402
r_{CC} (Å)			1.249	1.250	1.229	1.236	1.223
r_{CC} (Å)				1.337	1.369	1.361	1.383
r_{CC} (Å)					1.256	1.262	1.236
r_{CC} (Å)						1.325	1.361
r_{CC} (Å)							1.260
r_{CS} (Å)	1.573	1.560	1.627	1.565	1.616	1.568	1.612
θ_{CCS} (deg)	141.5	180	180	180	180	180	180
a_{eff}[a] (MHz)	11.3	22.7	9.0	15.4	6.1	10.8	4.8
μ (D)	2.49	2.68	2.97	3.21	3.36	3.63	3.59
μ_{ROHF} (D)	2.17	2.51	3.34	3.03	3.71	3.34	3.95
$\langle S^2 \rangle_{UHF}$	1.46	1.49	1.42	1.95	1.95	2.47	2.48

[a] $a_{eff} = a \pm (b + c)/2$, where $\pm$ refers to chains with odd and even numbers of carbon atoms, respectively.

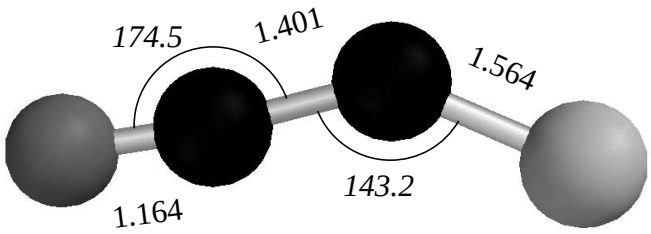

FIG. 1.—Molecular geometry of NCCS calculated at the QCISD/cc-pVDZ level of theory. Bond lengths are in Angstroms, and bond angles are in degrees.

integer quantum numbers. A search covering a frequency range of ±2% was then undertaken, and within 1% of the predicted frequencies, a series of strong, closely spaced magnetic lines was detected and assigned to the $K_a = 0$ level of NCCS on the basis of chemical assays and other tests. Conclusive confirmation of this assignment was finally provided by detection of the more abundant rare isotopic species.

The optimal experimental conditions for the present radicals were found to be similar to those that produce strong lines of the nitrogen-bearing radicals C_nN and the isovalent sulfur-bearing radicals HC_nS: a low-current dc discharge of 1300–1600 V synchronized with a 300–480 μs long gas pulse at a total pressure behind the nozzle of 2.5 ktorr (3.2 atm) and a total gas flow of 25–35 sccm (standard cubic centimeters per minute). With a precursor gas mixture of 0.6% cyanoacetylene (HCCCN) and 0.1% carbon disulfide (CS_2) in Ne, lines of the known radicals NCS (Amano & Amano 1991) and HC_4S (Hirahara, Ohshima, & Endo 1994) were readily observed. As was done for the HC_nS radicals, these experimental conditions were used in initial searches for the longer NC_nS chains; once found, the production of each radical was then optimized individually. The best conditions for the longer chains were very similar to those that optimize the shorter ones, except with slightly higher discharge voltage, increasing by about 100 V for each additional carbon atom.

The spectroscopic and chemical evidence for the assignments here is extremely good. For NC_3S and the four longer chains, the experimental rotational constants are larger than those predicted ab initio by about 3%, and for NCCS, $(B + C)/2$ of 2829 MHz is 0.8% larger than the theoretical result of 2807 MHz. The systematic underestimate of the computed rotational constants is consistent with vibrational effects, i.e., bending motion causes the vibrationally averaged experimental geometries to be more compact than the equilibrium geometries. The centrifugal distortion constants D_J of NC_3S and the four longer molecules in the sequence are also close to those expected from the isovalent HC_nS species. The absence of lines at subharmonic frequencies indicates that the carriers of the observed lines cannot be from larger or heavier molecules, and because the lines are harmonically related by half-integer (or integer for NCCS) quantum numbers, the carriers of the assigned lines are radicals. In addition, the rotational spectra of all six chains exhibit hyperfine structure that arises from the interaction of the nuclear spin with the unpaired electron; of the linear chains, all but NC_3S, NC_5S, and NC_7S have resolvable splittings owing to lambda-doubling in a $^2\Pi$ state.

The observed lines also pass several other tests: they are only found in the presence of an electrical discharge through gases containing both nitrogen and sulfur. The behavior of the observed lines in the presence of a magnetic field is also consistent with the assigned ground state of each molecule: lines of NC_4S and NC_6S are not modulated by a magnetic field of a few G, confirming that the ground state does not possess a large magnetic moment—as expected for a $^2\Pi_{1/2}$ state near the Hund's coupling case (a) limit. Lines of NC_3S and the two longer chains with an odd number of carbon atoms, however, are readily modulated with the same magnetic field, as expected for radicals with $^2\Pi_{3/2}$ ground states; lines of NCCS behave in a similar way, as expected for a molecule with a $^2A'$ ground state. Definitive confirmation of the NCCS assignment is provided by isotopic substitution: lines of each of the four isotopic species were observed within 0.2% of those calculated from the theoretical structure. For NC_3S, NC_4S, and NC_5S, lines of the ^{34}S species were also found within 0.1% of the predicted frequencies.

3. RESULTS AND ANALYSIS

3.1. *The* $NC_{2n}S$ *Sequence:* NC_4S *and* NC_6S

Each of the lower rotational transitions of NC_4S and NC_6S is split into six components by widely spaced lambda-doubling and closely spaced hfs from the spin 1 nitrogen nucleus. At least seven rotational transitions of both radicals fall within the frequency range of the FTM spectrometer; these and those of $NC_4^{34}S$ are given in Tables 2, 3, and 4. A sample FTM spectrum of NC_4S is shown in Figure 2*a*. A standard effective Hamiltonian for a molecule in a $^2\Pi$ electronic state (Brown et al. 1979; Amiot, Maillard, & Chauville 1981, Brown & Schubert 1982) was fitted to the measured transitions. With the fine-structure constant A constrained at 44 cm^{-1} (the HC_3S value; Hirahara et al. 1994), at most six spectroscopic constants—the rotational constant B, centrifugal distortion D, two lambda-doubling constants $p + 2q$ and $(p + 2q)_D$, and two hyperfine constants, the diagonal term $a_- = a - (b + c)/2$ and the parity-dependent term d—were required to reproduce the data to an accuracy of better than 3 kHz for each species. The spectroscopic constants derived for both radicals and $NC_4^{34}S$ are summarized in Tables 5 and 6, respectively.

3.2. *The* $NC_{2n+1}S$ *Sequence:* NCS, NC_3S, NC_5S, *and* NC_7S

Although a number of rotational transitions of NC_3S and the longer chains here are accessible with our FTM spectrometer, because of the large rotational constant of NCS, only its three lowest rotational transitions ($J' \leq 3.5$; Table 7), two in the $^2\Pi_{1/2}$ ladder and one in the $^2\Pi_{3/2}$ ladder, fall below the high-frequency cutoff (42 GHz) of the instrument. Somewhat surprisingly, transitions from both fine-structure states were observed in the generally rotationally cold molecular beam (T_{rot} = 2–3 K), even though the $^2\Pi_{1/2}$ rotational ladder lies about 450 K above the $^2\Pi_{3/2}$ ladder. By constraining the fine-structure constant A_{SO} and the lambda-doubling constant q to the values derived previously from the millimeter-wave data (Amano & Amamo 1991), it was possible to reproduce the centimeter-wave frequencies to better than 3 kHz by varying nine spectroscopic constants in the $^2\Pi$ Hamiltonian: B, D, two lambda-doubling constants [$p + 2q$ and $(p + 2q)_D$], and five hyperfine coupling constants (a, b, $b + c$, d and eQq); if b is constrained to zero, the fit rms increases by nearly a factor of 2. The derived NCS constants (see Table 8) are in good

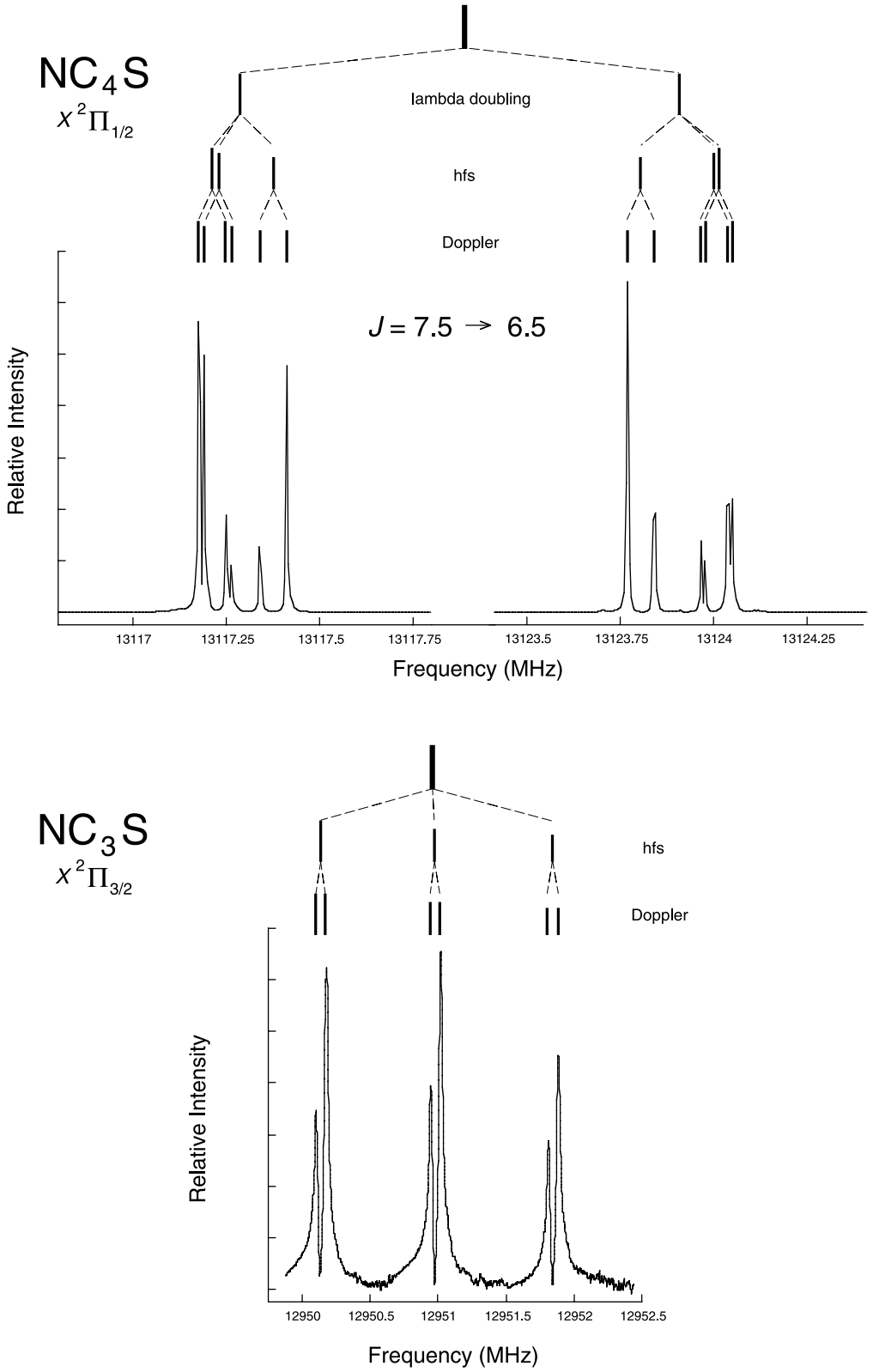

FIG. 2.—Sample spectra of NC_4S and NC_3S showing hfs and Doppler splitting. For NC_4S, Λ-doubling is well-resolved, but for NC_3S no such splitting is observed at our instrumental resolution of 10 kHz. The double-peaked line profile is an instrumental artifact: Doppler splitting results from the interaction of the supersonic axial molecular beam with the standing wave of the confocal Fabry-Perot microwave cavity. The integration time for each spectrum was approximately 2 minutes.

TABLE 2

MEASURED ROTATIONAL TRANSITIONS OF NC_4S IN THE $X\,^2\Pi_{1/2}$ STATE

Transition		e/f	Frequency	$O-C$
$J \rightarrow J'$	$F \rightarrow F'$	Λ Comp.[a]	(MHz)	(kHz)
4.5 → 3.5	5.5 → 4.5	*e*	7868.752	−2
	4.5 → 3.5	*e*	7868.793	1
	3.5 → 2.5	*e*	7869.188	2
	5.5 → 4.5	*f*	7875.545	0
	4.5 → 3.5	*f*	7876.168	2
	3.5 → 2.5	*f*	7876.193	3
5.5 → 4.5	6.5 → 5.5	*e*	9618.285	1
	5.5 → 4.5	*e*	9618.308	0
	4.5 → 3.5	*e*	9618.580	−1
	6.5 → 5.5	*f*	9624.965	0
	5.5 → 4.5	*f*	9625.358	−1
	4.5 → 3.5	*f*	9625.375	−1
6.5 → 5.5	7.5 → 6.5	*e*	11367.763	0
	6.5 → 5.5	*e*	11367.780	0
	5.5 → 4.5	*e*	11367.978	−2
	7.5 → 6.5	*f*	11374.380	1
	6.5 → 5.5	*f*	11374.653	0
	5.5 → 4.5	*f*	11374.663	−2
7.5 → 6.5	8.5 → 7.5	*e*	13117.216	2
	7.5 → 6.5	*e*	13117.229	3
	6.5 → 5.5	*e*	13117.379	0
	8.5 → 7.5	*f*	13123.792	1
	7.5 → 6.5	*f*	13123.989	−2
	6.5 → 5.5	*f*	13123.999	−2
8.5 → 7.5	9.5 → 8.5	*e*	14866.647	0
	8.5 → 7.5	*e*	14866.657	1
	7.5 → 6.5	*e*	14866.775	−2
	9.5 → 8.5	*f*	14873.199	0
	8.5 → 7.5	*f*	14873.356	4
	7.5 → 6.5	*f*	14873.356	−4
9.5 → 8.5	10.5 → 9.5	*e*	16616.066	−2
	9.5 → 8.5	*e*	16616.066	−9
	8.5 → 7.5	*e*	16616.171	−2
	10.5 → 9.5	*f*	16622.606	2
	9.5 → 8.5	*f*	16622.724	−1
	8.5 → 7.5	*f*	16622.724	−7
10.5 → 9.5	11.5 → 10.5	*e*	18365.488	9
	10.5 → 9.5	*e*	18365.488	4
	9.5 → 8.5	*e*	18365.563	−2
	11.5 → 10.5	*f*	18372.006	0
	10.5 → 9.5	*f*	18372.106	2
	9.5 → 8.5	*f*	18372.106	−3
11.5 → 10.5	12.5 → 11.5	*e*	20114.887	5
	11.5 → 10.5	*e*	20114.887	0
	10.5 → 9.5	*e*	20114.952	−2
	12.5 → 11.5	*f*	20121.407	2
	11.5 → 10.5	*f*	20121.487	1
	10.5 → 9.5	*f*	20121.487	−3
12.5 → 11.5	13.5 → 12.5	*e*	21864.285	7
	12.5 → 11.5	*e*	21864.285	3
	11.5 → 10.5	*e*	21864.340	0
	13.5 → 12.5	*f*	21870.800	0
	12.5 → 11.5	*f*	21870.868	0
	11.5 → 10.5	*f*	21870.868	−4

NOTES.—Estimated 1 σ measurement uncertainty is 2 kHz for isolated lines and 5 kHz for blended lines. Calculated frequencies were derived from the best-fit constants in Table 5.

[a] Designation of *e* and *f* levels is based on the assumption that the hyperfine constant *d* is positive.

TABLE 3

MEASURED ROTATIONAL TRANSITIONS OF NC_6S IN THE $X\,^2\Pi_{1/2}$ STATE

Transition		e/f	Frequency	$O-C$
$J \rightarrow J'$	$F \rightarrow F'$	Λ Comp.[a]	(MHz)	(kHz)
9.5 → 8.5	10.5 → 9.5	*e*	7511.785	−2
	9.5 → 8.5	*e*	7511.785	−3
	8.5 → 7.5	*e*	7511.842	4
	10.5 → 9.5	*f*	7514.620	−2
	9.5 → 8.5	*f*	7514.685	2
	8.5 → 7.5	*f*	7514.685	0
10.5 → 9.5	11.5 → 10.5	*e*	8302.660	0
	10.5 → 9.5	*e*	8302.660	−1
	9.5 → 8.5	*e*	8302.702	−1
	11.5 → 10.5	*f*	8305.489	2
	10.5 → 9.5	*f*	8305.539	2
	9.5 → 8.5	*f*	8305.539	1
12.5 → 11.5	13.5 → 12.5	*e*	9884.401	2
	12.5 → 11.5	*e*	9884.401	1
	11.5 → 10.5	*e*	9884.428	−2
	13.5 → 12.5	*f*	9887.216	1
	12.5 → 11.5	*f*	9887.248	−1
	11.5 → 10.5	*f*	9887.248	−2
13.5 → 12.5	14.5 → 13.5	*e*	10675.267	1
	13.5 → 12.5	*e*	10675.267	0
	12.5 → 11.5	*e*	10675.290	−3
	14.5 → 13.5	*f*	10678.077	−1
	13.5 → 12.5	*f*	10678.108	1
	12.5 → 11.5	*f*	10678.108	0
14.5 → 13.5	15.5 → 14.5	*e*	11466.135	3
	14.5 → 13.5	*e*	11466.135	2
	13.5 → 12.5	*e*	11466.155	0
	15.5 → 14.5	*f*	11468.939	−1
	14.5 → 13.5	*f*	11468.964	−2
	13.5 → 12.5	*f*	11468.964	−2
15.5 → 14.5	16.5 → 15.5	*e*	12256.997	1
	15.5 → 14.5	*e*	12256.997	0
	14.5 → 13.5	*e*	12257.017	0
	16.5 → 15.5	*f*	12259.802	0
	15.5 → 14.5	*f*	12259.823	−1
	14.5 → 13.5	*f*	12259.823	−2
16.5 → 15.5	17.5 → 16.5	*e*	13047.861	2
	16.5 → 15.5	*e*	13047.861	1
	17.5 → 16.5	*f*	13050.664	0
	16.5 → 15.5	*f*	13050.681	−1
	15.5 → 14.5	*f*	13050.681	−2
17.5 → 16.5	18.5 → 17.5	*e*	13838.723	2
	17.5 → 16.5	*e*	13838.723	1
	18.5 → 17.5	*f*	13841.523	0
	17.5 → 16.5	*f*	13841.542	2
	16.5 → 15.5	*f*	13841.542	1
18.5 → 17.5	19.5 → 18.5	*e*	14629.583	1
	18.5 → 17.5	*e*	14629.583	0
	18.5 → 17.5	*f*	14632.397	−1
	17.5 → 16.5	*f*	14632.397	−1
19.5 → 18.5	20.5 → 19.5	*e*	15420.442	0
	19.5 → 18.5	*e*	15420.442	0
	20.5 → 19.5	*f*	15423.241	0
	19.5 → 18.5	*f*	15423.254	0
	18.5 → 17.5	*f*	15423.254	−1

NOTES.—Estimated 1 σ measurement uncertainty is 2 kHz for isolated lines and 5 kHz for blended lines. Calculated frequencies were derived from the best-fit constants in Table 5.

[a] Designation of *e* and *f* levels is based on the assumption that the hyperfine constant *d* is positive.

TABLE 4
MEASURED ROTATIONAL TRANSITIONS OF $NC_4^{34}S$ IN THE $X\,^2\Pi_{1/2}$ STATE

Transition		e/f	Frequency	$O-C$
$J \rightarrow J'$	$F \rightarrow F'$	Λ Comp.[a]	(MHz)	(kHz)
5.5 → 4.5	6.5 → 5.5	e	9375.549	2
	5.5 → 4.5	e	9375.569	−2
	4.5 → 3.5	e	9375.843	1
	6.5 → 5.5	f	9382.076	−2
	5.5 → 4.5	f	9382.468	−1
	4.5 → 3.5	f	9382.486	0
6.5 → 5.5	7.5 → 6.5	e	11080.880	2
	6.5 → 5.5	e	11080.895	0
	5.5 → 4.5	e	11081.093	0
7.5 → 6.5	8.5 → 7.5	e	12786.180	−2
	7.5 → 6.5	e	12786.194	0
	6.5 → 5.5	e	12786.344	−2
	8.5 → 7.5	f	12792.605	−1
	7.5 → 6.5	f	12792.806	1
	6.5 → 5.5	f	12792.816	2
8.5 → 7.5	9.5 → 8.5	e	14491.469	1
	8.5 → 7.5	e	14491.478	1
	7.5 → 6.5	e	14491.594	−3
	9.5 → 8.5	f	14497.865	0
	8.5 → 7.5	f	14498.015	−2
	7.5 → 6.5	f	14498.025	0
9.5 → 8.5	10.5 → 9.5	e	16196.739	−3
	9.5 → 8.5	e	16196.739	−10
	8.5 → 7.5	e	16196.847	1
	10.5 → 9.5	f	16203.126	4
	9.5 → 8.5	f	16203.244	2
	8.5 → 7.5	f	16203.244	−4
10.5 → 9.5	11.5 → 10.5	e	17902.003	−3
	10.5 → 9.5	e	17902.003	−9
	9.5 → 8.5	e	17902.098	6
	11.5 → 10.5	f	17908.378	4
	10.5 → 9.5	f	17908.474	3
	9.5 → 8.5	f	17908.474	−2
11.5 → 10.5	12.5 → 11.5	e	19607.267	4
	11.5 → 10.5	e	19607.267	−1
	10.5 → 9.5	e	19607.334	−1
	12.5 → 11.5	f	19613.618	−5
	11.5 → 10.5	f	19613.708	4
	10.5 → 9.5	f	19613.708	0

NOTES.—Estimated 1 σ measurement uncertainty is 2 kHz for isolated lines and 5 kHz for blended lines. Calculated frequencies were derived from the best-fit constants in Table 6.

[a] Designation of e and f levels is based on the assumption that the hyperfine constant d is positive.

agreement with those previously reported by Amano & Amano (1991).

Hyperfine structure was also observed in the lower rotational transitions of NC_3S, NC_5S, and NC_7S, but lambda-doubling was unresolved at our instrumental resolution of 10 kHz. The measured transition frequencies are given in Tables 9, 10, and 11, those of $NC_3^{34}S$ and $NC_5^{34}S$ are given in Tables 12 and 13, and a sample spectra of NC_3S is shown in Figure 2*b*. The measurements were analyzed in the same way as the NC_4S and NC_6S data, except the fine-structure constant A was constrained to -327 cm^{-1} (i.e., the NCS value). Three parameters were required to reproduce the experimental data to a rms of better than 3 kHz for each molecule: B, D, and the hyperfine coupling constant, $a_+ = a + (b + c)/2$. The magnitude of the NC_3S lambda-doubling constant q is expected to be extremely small by extrapolation from NCS; the lack of any splitting at our instrumental resolution implies that $q \leq 0.2$ MHz—an upper limit that is roughly two and one-half times larger than $q \sim 0.08$ MHz expected by extrapolation (i.e., the q of NCS scaled by the ratio of the rotational constant of NC_3S to that of NCS). The spectroscopic constants of these three longer chains are summarized in Table 14; constants for the ^{34}S isotopic species are given in Table 6.

4. DISCUSSION

A structural anomaly is immediately apparent in the molecules studied here: NCCS is bent, but NCS and the five longer homologous chains with both odd and even numbers of carbon atoms up to NC_7S have linear (or nearly linear) heavy-atom backbones. All of the closely related HC_nS chains up to HC_8S (Gordon et al. 2002) except HCS (Habara, Yamamoto, & Amano 2002) are also known to be linear. In contrast, rotational studies of the HC_nO chains up to HC_4O demonstrate that all of these molecules are significantly nonlinear, with the two longer chains possessing bent carbon-chain backbones which depart from linearity by about 20° (Cooksy et al. 1994; Kohguchi, Ohshima, & Endo 1994).

Only NCCS and NC_4S are predicted to have nonlinear equilibrium geometries in ROHF/cc-pVDZ geometry optimizations of the NC_nS sequence to $n = 7$. These geometries can be understood in terms of a simple structural argument: bending the chain tends to localize the unpaired electron in an sp^2 hybrid orbital and disrupts the π system conjugation in the plane of the bend. Breaking the conjugation is destabilizing, but localizing the unpaired electron often compensates by increasing the s character of its orbital, increasing the electron-nuclear interaction of that orbital. Bending the CCS chain in the plane of the unpaired electron orbital tends to stabilize the radical when n is even, because the unpaired electron is localized near the end of the chain, minimizing any impact on the conjugation. However, conjugation becomes more important as the chain length increases because the highest occupied molecular orbital (HOMO) has less antibonding character in the longer chains (the number of nodes increases half as fast as the chain length). Consequently, the predicted barrier to linearity in NC_4S is only 2 kJ mol^{-1} at the ROHF level, compared to 16 kJ mol^{-1} for NCCS, and UHF and UQCISD calculations predict NC_4S to be linear. In NC_6S, the HOMO has about the same energy in the bent and linear configurations, and ROHF and UHF predictions agree that the structure should be linear.

The odd NC_nS species have less tendency to bend, regardless of chain length, because bending tends to localize the unpaired electron toward the middle of the carbon chain. Bending the CCS subunit imposes a C—Ċ═S bond distribution on those atoms, but when n is odd the CC bond tends toward triple, rather than single, bond character. No satisfactory canonical structure exists with a nonlinear CCS angle when n is odd. Although satisfactory structures can be drawn when the chains are bent at more central carbon atoms, these suffer greater loss of in-plane conjugation, and the linear structure remains more stable.

A comparative experimental and theoretical study of nitrogen-oxygen, nitrogen-sulfur, and closely related carbon chains might be useful to clarify the relative importance

TABLE 5
SPECTROSCOPIC CONSTANTS OF NC_4S AND NC_6S (IN MHz)

	NC_4S		NC_6S	
CONSTANT	Measured	Expected	Measured	Expected
A	1,328,800[a]		1,328,800[a]	
B	875.28450(5)	848[c]	395.55133(5)	383[c]
$10^6 D$	14.2(2)	12.3[d]	2.0(1)	1.5[e]
$p + 2q$	6.413(2)		2.787(2)	
$10^3(p + 2q)_D$	0.119(7)		...	
$a - (b + c)/2$	11.88(3)	15.4[c]	6.6(2)	10.8[c]
d	18.35(7)		9.7(5)	
eQq	−4.06[b]		−4.06[b]	

NOTES.—Uncertainties (in parentheses) are 1 σ in the last significant digit. The spin-rotation constant γ was constrained to zero in each fit.
[a] Constrained to HC_3S value (McCarthy et al. 1997).
[b] Constrained to NCS value (see Table 8).
[c] Computed at the QCISD/cc-pVDZ level of theory (see Table 1).
[d] HC_5S value (Gordon et al. 2002).
[e] HC_7S value (Gordon et al. 2002).

that π conjugation, hybridization, atomic properties (e.g., radius, spin orbit), etc., play in determining molecular structure and chemical bonding. Apparently, the interplay between these effects is somewhat subtle since only NCCS is known experimentally to possess a bent ground state geometry. NCO, isovalent to NCS, has been studied by microwave and far-infrared laser magnetic resonance spectroscopy (Saito & Amano 1970; Davies & Davis 1990), but there is no comparable information on NCCO or longer chains, even though NCCO has been the subject of several theoretical (Cooksy 1995; Francisco & Liu 1997; Jursic 1999) and experimental studies (Ramsay & Winnewisser 1983; Furlan, Scheld, & Huber 1998). Laboratory studies of NC_nO and longer HC_nO chains should be possible, especially given the ready availability of precursor gases (e.g., O_2, CO, CO_2) analogous to those used here to produce strong lines of sulfur-bearing chains.

All of the new molecules here probably possess strong electronic transitions in the visible. NCS has been studied at optical wavelengths by a variety of laser techniques (Ohtoshi et al. 1984; Northrup & Sears 1990), and the HC_nS chains up to HC_6S have been studied by laser-induced fluorescence by Endo and coworkers (Nakajima, Sumiyoshi, & Endo 2002). Taking into account differences in the rotational partition function and dipole moments, the present nitrogen-sulfur carbon chains are produced with comparable abundance to the HC_nS chains of the same length in our discharge source in sufficient abundance ($>10^8$ molecules/pulse) so that their optical spectra may be detectable with present laser techniques (i.e., cavity ringdown spectroscopy, laser-induced fluorescence, or two-color, two-photon, resonant-enhanced ionization spectroscopy).

It is also worth noting that rotational transitions from the upper fine-structure state of NCS, several hundred Kelvin above ground, are readily detected in our rotationally cold molecular beam. Rotational transitions from vibrationally excited states of diatomic and polyatomic molecules (Sanz, McCarthy, & Thaddeus, 2003, in preparation) have also been observed in the same discharge source, which suggests that relaxation between fine-structure ladders may be mediated by the same or similar relaxation processes, i.e., collisionally induced cooling. Because NCS is very close to the Hund's case (a) limit, radiative relaxation occurs on a longer timescale than

TABLE 6
SPECTROSCOPIC CONSTANTS OF $NC_3^{34}S$, $NC_4^{34}S$, AND $NC_5^{34}S$ (IN MHz)

	$NC_3^{34}S$		$NC_4^{34}S$		$NC_5^{34}S$	
CONSTANT	Measured	Expected	Measured	Expected	Measured	Expected
A	−9,820,900[a]		1,328,800[a]		−9,820,900[a]	
B	1402.3182(1)	1402.3[b]	853.1818(6)	853.2[b]	554.9469(8)	554.9[b]
$10^6 D$	43.2(7)	44.6[b]	14.2(4)	13.5[b]	4.4(2)	4.5[b]
$p + 2q$			6.270(4)	6.25[b]		
$10^3(p + 2q)_D$			0.07(1)			
$a - (b + c)/2$			11.79(4)	11.88[c]	...	...
$a + (b + c)/2$	11.44(1)	11.43[c]	...	...	5.75(5)	5.76[c]
d	...	...	18.2(1)	18.35[c]	...	...
eQq	−4.23[a]	...	−4.06[a]	...	−4.23[a]	...

NOTES.—Uncertainties (in parentheses) are 1 σ in the last significant digit. The spin-rotation constant γ was constrained to 0 in each fit.
[a] Constrained to value of normal isotopic species.
[b] Scaled from normal isotopic species.
[c] Value measured in normal isotopic species.

TABLE 7

Measured Rotational Transitions of NCS in the $X\,^2\Pi_i$ State

Transition					
$J \rightarrow J'$	$F \rightarrow F'$	Ω	e/f Λ Comp.[a]	Frequency (MHz)	$O-C$ (kHz)
1.5 → 0.5	2.5 → 1.5	1/2	e	18192.892	0
	1.5 → 0.5		e	18200.075	−2
	1.5 → 1.5		e	18207.414	−1
	0.5 → 0.5		e	18211.250	2
	1.5 → 1.5		f	18439.249	1
	2.5 → 1.5		f	18476.982	−1
	0.5 → 0.5		f	18490.134	−2
	1.5 → 0.5		f	18510.427	2
2.5 → 1.5	3.5 → 2.5	1/2	e	30422.628	1
	2.5 → 1.5		e	30424.061	−2
	1.5 → 0.5		e	30426.922	1
	3.5 → 2.5		e	30703.702	1
	2.5 → 1.5		f	30710.346	−1
	1.5 → 0.5		f	30710.994	−1
2.5 → 1.5	3.5 → 2.5	3/2	e	30497.135	−3
	3.5 → 2.5		f	30497.155	3
	2.5 → 1.5		e	30505.691	−2
	2.5 → 1.5		f	30505.709	2
	1.5 → 0.5		e	30512.180	−3
	1.5 → 0.5		f	30512.200	3

Notes.—Estimated 1 σ measurement uncertainty: 2 kHz, except for the rotational transitions in the $\Omega = 3/2$ ladder, whose estimated uncertainties are 5 kHz. Calculated frequencies were derived from the best-fit constants in Table 8.

[a] Designation of e and f levels is based on the assumption that the sign of the hyperfine constant d is positive.

molecular expansion (of order 1 ms) and therefore is probably negligible. Recently, Kim, Habara, & Yamamoto (2002) detected rotational transitions from both fine-structure ladders of isovalent HCCS using a similar spectrometer to ours. Rotational transitions from the upper fine-structure level of C_6H ($^2\Pi_{1/2}$; $A_{SO} = 15$ cm^{-1}) have also been observed in this laboratory, but the lines are quite weak, possibly owing to a shorter radiative lifetime. It is unclear if hyperfine-split lines from higher-lying fine-structure ladders of other molecules can now be observed in our molecular beam; radicals with $^2\Pi$

TABLE 8

Spectroscopic Constants of NCS (in MHz)

Constant	This Work	Amano & Amano 1991
A	−9,820,900[a]	−9,820,900
B	6106.6243(7)	6106.62162(25)
$10^6 D$	1769(52)	1769.51(17)
γ_{eff}	−3632.56[a]	−3632.56(11)
$p + 2q$	278.916(4)	278.994(31)
$10^3(p + 2q)_D$	−2.9(3)	−1.4874(87)
q	−0.35818[a]	−0.35818(37)
a	28.313(3)	
b	5.2(10)	
$b + c$	−7.256(7)	
d	39.238(3)	
$a + (b + c)/2$	...	26.06(23)
eQq	−4.063(4)	−3.26(83)

Note.—Uncertainties (in parentheses) are 1 σ in the last significant digit.

[a] Fixed to value derived from millimeter-wave study (Amano & Amano 1991).

TABLE 9

Measured Rotational Transitions of NC_3S in the $X\,^2\Pi_{3/2}$ State

Transition[a]		Frequency (MHz)	$O-C$ (kHz)
$J \rightarrow J'$	$F \rightarrow F'$		
2.5 → 1.5	3.5 → 2.5	7193.206	6
3.5 → 2.5	4.5 → 3.5	10071.864	0
	3.5 → 2.5	10073.333	7
	2.5 → 1.5	10075.025	7
4.5 → 3.5	5.5 → 4.5	12950.140	−2
	4.5 → 3.5	12950.988	−2
	3.5 → 2.5	12951.922	0
5.5 → 4.5	6.5 → 5.5	15828.262	−2
	5.5 → 4.5	15828.820	1
	4.5 → 3.5	15829.415	−1
6.5 → 5.5	7.5 → 6.5	18706.308	2
	6.5 → 5.5	18706.701	2
	5.5 → 4.5	18707.118	2
7.5 → 6.5	8.5 → 7.5	21584.304	1
	7.5 → 6.5	21584.596	0
	6.5 → 5.5	21584.900	−4
8.5 → 7.5	9.5 → 8.5	24462.270	2
	8.5 → 7.5	24462.497	1
	7.5 → 6.5	24462.730	−3

Notes.—Estimated 1 σ measurement uncertainty: 2 kHz, except for the lowest two rotational transitions, whose estimated uncertainties are 5 kHz. Calculated frequencies were derived from the best-fit constants in Table 14.

[a] Lambda-doubling unresolved in the $^2\Pi_{3/2}$ fine-structure ladder.

TABLE 10

Measured Rotational Transitions of NC_5S in the $X\,^2\Pi_{3/2}$ State

Transition[a]		Frequency (MHz)	$O-C$ (kHz)
$J \rightarrow J'$	$F \rightarrow F'$		
5.5 → 4.5	6.5 → 5.5	6258.839	0
	5.5 → 4.5	6259.049	−2
	4.5 → 3.5	6259.413	3
6.5 → 5.5	7.5 → 6.5	7396.894	2
	6.5 → 5.5	7397.046	−2
	5.5 → 4.5	7397.292	2
7.5 → 6.5	8.5 → 7.5	8534.929	0
	7.5 → 6.5	8535.048	1
	6.5 → 5.5	8535.221	−1
8.5 → 7.5	9.5 → 8.5	9672.956	2
	8.5 → 7.5	9673.048	0
	7.5 → 6.5	9673.179	−1
9.5 → 8.5	10.5 → 9.5	10810.972	0
	9.5 → 8.5	10811.048	0
	8.5 → 7.5	10811.151	−1
10.5 → 9.5	11.5 → 10.5	11948.985	0
	10.5 → 9.5	11949.049	1
	9.5 → 8.5	11949.131	0
11.5 → 10.5	12.5 → 11.5	13086.995	1
	11.5 → 10.5	13087.045	−2
	10.5 → 9.5	13087.116	1
12.5 → 11.5	13.5 → 12.5	14225.000	0
	12.5 → 11.5	14225.046	1
	11.5 → 10.5	14225.101	−1
13.5 → 12.5	14.5 → 13.5	15363.004	1
	13.5 → 12.5	15363.042	0
	12.5 → 11.5	15363.089	−1

TABLE 10—*Continued*

Transition[a]		Frequency (MHz)	$O-C$ (kHz)
$J \rightarrow J'$	$F \rightarrow F'$		
14.5 → 13.5.....	15.5 → 14.5	16501.003	0
	14.5 → 13.5	16501.037	0
	13.5 → 12.5	16501.077	−2
15.5 → 14.5.....	16.5 → 15.5	17639.001	0
	15.5 → 14.5	17639.029	−2
	14.5 → 13.5	17639.066	−1
16.5 → 15.5.....	17.5 → 16.5	18776.996	0
	16.5 → 15.5	18777.022	0
	15.5 → 14.5	18777.054	0
17.5 → 16.5.....	18.5 → 17.5	19914.990	1
	17.5 → 16.5	19915.014	2
	16.5 → 15.5	19915.039	−1
18.5 → 17.5.....	19.5 → 18.5	21052.980	1
	18.5 → 17.5	21053.002	1
	17.5 → 16.5	21053.024	−2

Notes.—Estimated 1 σ measurement uncertainty is 2 kHz. Calculated frequencies were derived from the best-fit constants in Table 14.

[a] Lambda-doubling unresolved in the $^2\Pi_{3/2}$ fine-structure ladder.

electronic ground states and comparably large spin-orbit coupling constants to NCS and HCCS would appear to be good candidates for further study.

Members of the NC_nS family are also good candidates for detection by radio astronomers. NCS is highly polar, and we calculate that NCCS and longer chains are equally polar or more so, with dipole moments ranging from 2 D to almost 4 D (see Table 1). The closely related C_nS and C_nN chains up to C_3S and C_5N are well-known astronomical molecules, as are the simple nitrogen-sulfur molecules NS and HNCS, implying that with dedicated searches other nitrogen-sulfur carbon chains might be detected in rich

TABLE 11

Measured Rotational Transitions of NC_7S in the $X\,^2\Pi_{3/2}$ State

Transition[a]		Frequency (MHz)	$O-C$ (kHz)
$J \rightarrow J'$	$F \rightarrow F'$		
15.5 → 14.5	16.5 → 15.5	8834.061	0
	15.5 → 14.5	8834.072	0
	14.5 → 13.5	8834.092	0
16.5 → 15.5	17.5 → 16.5	9404.000	−1
	16.5 → 15.5	9404.013	2
	15.5 → 14.5	9404.028	0
17.5 → 16.5	18.5 → 17.5	9973.940	0
	17.5 → 16.5	9973.952	3
	16.5 → 15.5	9973.963	−1
18.5 → 17.5	19.5 → 18.5	10543.879	0
	18.5 → 17.5	10543.888	1
	17.5 → 16.5	10543.897	−3
19.5 → 18.5	20.5 → 19.5	11113.816	−1
	19.5 → 18.5	11113.827	2
	18.5 → 17.5	11113.835	−1
20.5 → 19.5	21.5 → 20.5	11683.754	0
	20.5 → 19.5	11683.763	2
	19.5 → 18.5	11683.772	0
21.5 → 20.5	22.5 → 21.5	12253.690	−1
	21.5 → 20.5	12253.698	0
	20.5 → 19.5	12253.708	1

Notes.—Estimated 1 σ measurement uncertainty is 2 kHz. Calculated frequencies were derived from the best-fit constants in Table 14.

[a] Lambda-doubling unresolved in the $^2\Pi_{3/2}$ fine-structure ladder.

TABLE 12

Measured Rotational Transitions of $NC_3^{34}S$ in the $X\,^2\Pi_{3/2}$ State

Transition[a]		Frequency (MHz)	$O-C$ (kHz)
$J \rightarrow J'$	$F \rightarrow F'$		
3.5 → 2.5	4.5 → 3.5	9813.866	0
	3.5 → 2.5	9815.335	7
	2.5 → 1.5	9817.022	0
4.5 → 3.5	5.5 → 4.5	12618.428	−3
	4.5 → 3.5	12619.281	3
	3.5 → 2.5	12620.210	−2
5.5 → 4.5	6.5 → 5.5	15422.838	−1
	5.5 → 4.5	15423.396	1
	4.5 → 3.5	15423.993	1
7.5 → 6.5	8.5 → 7.5	21031.454	1
	7.5 → 6.5	21031.748	1
	6.5 → 5.5	21032.052	−3
8.5 → 7.5	9.5 → 8.5	23835.710	3
	8.5 → 7.5	23835.934	0
	7.5 → 6.5	23836.169	−3

Notes.— Estimated 1 σ measurement uncertainty: 2 kHz, except for the lowest rotational transition, whose estimated uncertainty is 5 kHz. Calculated frequencies were derived from the best-fit constants in Table 6.

[a] Lambda-doubling unresolved in the $^2\Pi_{3/2}$ fine-structure ladder.

TABLE 13

Measured Rotational Transitions of $NC_5^{34}S$ in the $X\,^2\Pi_{3/2}$ State

Transition[a]		Frequency (MHz)	$O-C$ (kHz)
$J \rightarrow J'$	$F \rightarrow F'$		
9.5 → 8.5	10.5 → 9.5	10543.309	0
	9.5 → 8.5	10543.385	0
	8.5 → 7.5	10543.489	1
10.5 → 9.5	11.5 → 10.5	11653.145	−2
	10.5 → 9.5	11653.210	0
	9.5 → 8.5	11653.294	2
11.5 → 10.5	12.5 → 11.5	12762.980	−1
	11.5 → 10.5	12763.034	0
	10.5 → 9.5	12763.101	−1
12.5 → 11.5	13.5 → 12.5	13872.812	0
	12.5 → 11.5	13872.856	−1
	11.5 → 10.5	13872.912	−2
13.5 → 12.5	14.5 → 13.5	14982.642	2
	13.5 → 12.5	14982.678	−1
	12.5 → 11.5	14982.727	0
14.5 → 13.5	15.5 → 14.5	16092.468	2
	14.5 → 13.5	16092.499	0
	13.5 → 12.5	16092.540	−1

Notes.—Estimated 1 σ measurement uncertainty is 2 kHz. Calculated frequencies were derived from the best-fit constants in Table 6.

[a] Lambda-doubling unresolved in the $^2\Pi_{3/2}$ fine-structure ladder.

TABLE 14
SPECTROSCOPIC CONSTANTS OF NC_3S, NC_5S, AND NC_7S (IN MHz)

	NC_3S		NC_5S		NC_7S	
CONSTANT	Measured	Expected	Measured	Expected	Measured	Expected
A	−9,820,900[a]		−9,820,900[c]		−9,820,900[c]	
B	1439.18582(8)	1395[b]	569.03617(3)	551[b]	284.97883(6)	275.8[b]
$10^6 D$	45.8(8)	47[c]	4.68(7)	3.1[e]	0.89(8)	1.0[f]
$a + (b + c)/2$	11.429(8)	9.0[b]	5.76(2)	6.1[b]	2.9(1)	3[g]
eQq	−4.23(2)		−4.23[d]		−4.23[d]	

NOTE.—Uncertainties (in parentheses) are 1 σ in the last significant digit.
[a] Constrained to NCS value.
[b] Computed at the QCISD/cc-pVDZ level of theory.
[c] HC_4S value (Hirahara et al. 1994).
[d] Constrained to NC_3S value.
[e] HC_6S value (Gordon et al. 2002).
[f] HC_8S value (Gordon et al. 2002).
[g] Extrapolated from shorter NC_nS chains.

interstellar and circumstellar sources. C_2S (Saito et al. 1987) and C_3S (Yamamoto et al. 1987), for example, were shown to be the carriers of strong unidentified astronomical lines in IRC +10216 (Suzuki et al. 1984; Kaifu et al. 1987), the same source where strong lines of C_3N were also found by Guélin & Thaddeus (1977). In TMC-1, the same two carbon-sulfur chains are surprisingly abundant (Hirahara et al. 1992), and the C_3N/HC_3N ratio there of about 0.1 is comparable to that in IRC +10216. With the spectroscopic constants listed in Tables 5, 8, and 14, the astronomically most interesting lines to radio astronomers can be calculated to better than 1 km s^{-1} in equivalent radial velocity up to 100 GHz for all but the longest two chains here (NC_6S and NC_7S); for these, the radio lines can be predicted to the same level of accuracy up to 50 GHz. To assist radio astronomical searches we have also tabulated in Tables 15 and 16 the stronger

TABLE 15
CALCULATED ROTATIONAL TRANSITIONS OF NCS IN THE $X\,^2\Pi_{3/2}$ STATE IN THE 3 mm BAND

TRANSITION		e/f	FREQUENCY
$J \rightarrow J'$	$F \rightarrow F'$	Λ Comp.[a]	(MHz)
6.5 → 5.5	7.5 → 6.5	e	79300.46
		f	79300.56
	6.5 → 5.5	e	79301.41
		f	79301.51
	5.5 → 4.5	e	79302.23
		f	79302.33
7.5 → 6.5	8.5 → 7.5	e	91500.07
		f	91500.20
	7.5 → 6.5	e	91500.77
		f	91500.90
	6.5 → 5.5	e	91501.38
		f	91501.51
8.5 → 7.5	9.5 → 8.5	e	103699.30
		f	103699.47
	8.5 → 7.5	e	103699.84
		f	103700.00
	7.5 → 6.5	e	103700.32
		f	103700.48
9.5 → 8.5	10.5 → 9.5	e	115898.14
		f	115898.35
	9.5 → 8.5	e	115898.57
		f	115898.77
	8.5 → 7.5	e	115898.95
		f	115899.16
10.5 → 9.5	11.5 → 10.5	e	128096.56
		f	128096.81
	10.5 → 9.5	e	128096.90
		f	128097.15
	9.5 → 8.5	e	128097.21
		f	128097.46

NOTE.—Estimated 1 σ uncertainties are 1 ppm or less.
[a] Designation of e and f levels is based on the assumption that the hyperfine constant d is positive.

TABLE 16
CALCULATED ROTATIONAL TRANSITIONS OF NC_3S IN THE $X\,^2\Pi_{3/2}$ STATE IN THE 3 mm BAND

Transition	Frequency (MHz)
25.5 → 24.5	73384.69
26.5 → 25.5	76262.27
27.5 → 26.5	79139.82
28.5 → 27.5	82017.34
29.5 → 28.5	84894.83
30.5 → 29.5	87772.28
31.5 → 30.5	90649.70
32.5 → 31.5	93527.09
33.5 → 32.5	96404.44
34.5 → 33.5	99281.76
35.5 → 34.5	102159.04
36.5 → 35.5	105036.27
37.5 → 36.5	107913.47
38.5 → 37.5	110790.63
39.5 → 38.5	113667.74
40.5 → 39.5	116544.83
41.5 → 40.5	119421.84
42.5 → 41.5	122298.82
43.5 → 42.5	125175.76
44.5 → 43.5	128052.64
45.5 → 44.5	130929.48
46.5 → 45.5	133806.27

NOTE.—Estimated 1 σ uncertainties are 1 ppm or less. Hyperfine structure has not been included since the splittings are less than 0.1 km s^{-1}.

expected radio lines of NCS and NC_3S in the 3 mm band. Astronomical detection of carbon chains beyond NS would enable one to make more complete comparisons of the column densities of analogous sulfur- and oxygen-bearing molecules and would provide additional tests for gas-phase synthesis models of astronomical molecules.

Note added in manuscript.—Following completion of the present work, the HC_5O, HC_6O, and HC_7O carbon-chain radicals were detected by the same technique. In contrast to the shorter members in this sequence, these chains are all found to possess linear heavy-atom backbones and $^2\Pi$ electronic ground states. An account of these observations will be given elsewhere.

The authors thank A. J. Apponi for assistance with early experiments, J. Dudek for synthesis of precursor gases, and M. E. Sanz and C. A. Gottlieb for helpful discussions. The experimental portion of this research is supported by NASA grant NAG5-9379 and NSF grant AST-9820722, and the theoretical portion is supported by NSF grant CHE-0216563.

REFERENCES

Amano, T., & Amano, T. 1991, J. Chem. Phys., 95, 2275
Amiot, C., Maillard, J.-P., & Chauville, J. 1981, J. Mol. Spectrosc., 87, 196
Brown, J. M., Colbourn, E. A., Watson, J. K. G., & Wayne, F. D. 1979, J. Mol. Spectrosc., 74, 294
Brown, J. M., & Schubert, J. E. 1982, J. Mol. Spectrosc., 95, 194
Cooksy, A. L. 1995, J. Am. Chem. Soc., 117, 1098
———. 2001, J. Am. Chem. Soc., 123, 4003
Cooksy, A. L., Watson, J. K. G., Gottlieb, C. A., & Thaddeus, P. 1994, J. Chem. Phys., 101, 178
Davies, P. B., & Davis, I. H. 1990, Mol. Phys., 69, 175
Francisco, J. S., & Liu, R. 1997, J. Chem. Phys., 107, 3840
Frerking, M. A., Linke, R. A., & Thaddeus, P. 1979, ApJ, 234, L143
Frisch, M. J., et al. 1998, Gaussian 98, Rev. A.6 (Pittsburgh: Gaussian Inc.)
Furlan, A., Scheld, H. A., & Huber, J. R. 1998, Chem. Phys. Lett., 282, 1
Gordon, V. D., McCarthy, M. C., Apponi, A. J., & Thaddeus, P. 2001, ApJS, 134, 311
Gordon, V. D., McCarthy, M. C., Apponi, A. J., & Thaddeus, P. 2002, ApJS, 138, 297
Gottlieb, C. A., Ball, J. A., Gottlieb, E. W., Lada, C. J., & Penfield, H. 1975, ApJ, 200, L147
Guélin, M., Neininger, N., & Cernicharo, J. 1998, A&A, 335, L1
Guélin, M., & Thaddeus, P. 1977, ApJ, 212, L81
Habara, H., Yamamoto, S., & Amano, T. 2002, J. Chem. Phys., 116, 9232
Hirahara, Y., Ohshima, Y., & Endo, Y. 1994, J. Chem. Phys., 101, 7342
Hirahara, Y., et al. 1992, ApJ, 394, 539
Jursic, B. S. 1999, Theochem., 460, 207
Kaifu, N., Suzuki, H., Ohishi, M., Miyaji, T., Ishikawa, S., Kasuga, T., Morimoto, M., & Saito, S. 1987, ApJ, 317, L111
Kim, E., Habara, H., & Yamamoto, S. 2002, J. Mol. Spectrosc., 212, 83
Kohguchi, H., Ohshima, Y., & Endo, Y. 1994, J. Chem. Phys., 101, 6463
Kuiper, T. B. H., Zuckerman, B., Kakar, R. K., & Kuiper, E. N. R. 1975, ApJ, 200, L151
Lee, S. 1997, Chem. Phys. Lett., 268, 69
McCarthy, M. C., Chen, W., Travers, M. J., & Thaddeus, P. 2000, ApJS, 129, 611
McCarthy, M. C., Travers, M. J., Kovács, A., Gottlieb, C. A., & Thaddeus, P. 1997, ApJS, 113, 105
Nakajima, M., Sumiyoshi, Y., & Endo, Y. 2002, Chem. Phys. Lett., 355, 116
Northrup, F. J., & Sears, T. J. 1990, Mol. Phys., 71, 45
Ohtoshi, H., Tsukiyama, K., Yanagibori, A., Shibuya, K., Obi, K., & Tanaka, K. 1984, Chem. Phys. Lett., 111, 136
Parker, C. L., & Cooksy, A. L. 1999, J. Phys. Chem., A103, 2160
Ramsay, D., & Winnewisser, M. 1983, Chem. Phys. Lett., 96, 502
Saito, S., & Amano, T. 1970, J. Mol. Spectrosc., 34, 383
Saito, S., Kawaguchi, K., Yamamoto, S., Ohishi, M., Suzuki, H., & Kaifu, N. 1987, ApJ, 317, L115
Sanz, M. E., McCarthy, M. C., & Thaddeus, P. 2002, J. Chem. Phys., submitted
Schmidt, M. W., et al. 1993, J. Comput. Chem., 14, 1347
Suzuki, H., Kaifu, N., Miyaji, T., Morimoto, M., Ohishi, M., & Saito, S. 1984, ApJ, 282, 197
Wong, M. W., & Radom, L. 1995, J. Chem. Phys., 99, 8582
Yamamoto, S., Saito, S., Kawaguchi, K. Kaifu, N., Suzuki, H., & Ohishi, M. 1987, ApJ, 317, L119